water

MDPI

Article

Flood-Induced Agricultural Damage Assessment: A Case Study of Pakistan

Abid Nazir [1,*], Awais Ahmad [2], Mohsin Ramzan [3], Hammad Gilani [1,4], Muhammad Mobeen [5,6], Shahid Tarer [2] and Niall P. Hanan [1]

[1] Plant and Environmental Sciences, New Mexico State University, Las Cruces, NM 88003, USA; hammadgilani@gmail.com (H.G.); nhanan@nmsu.edu (N.P.H.)
[2] Department of Remote Sensing, Kashtkaar, Gujranwala 50030, Pakistan; awais.ahmad@kashtkaar.com (A.A.); shahid@kashtkaar.com (S.T.)
[3] Department of Urban and Regional Planning, University at Buffalo, Buffalo, NY 14260, USA; mohsinra@buffalo.edu
[4] School of Interdisciplinary Engineering and Sciences, National University of Sciences and Technology, Islamabad 44000, Pakistan
[5] Research Group Climate Change and Security (CLISEC), Institute of Geography, University of Hamburg, 20144 Hamburg, Germany; muhammad.mobeen@uni-hamburg.de
[6] School of Integrated Climate System Sciences (SICSS), University of Hamburg, 20144 Hamburg, Germany
* Correspondence: abid@nmsu.edu

Abstract

Climate variability and extreme weather events, particularly flooding, pose growing threats to agricultural productivity worldwide, including in Pakistan. Traditional crop damage assessments during flood events have relied on field surveys, which are often time-intensive and spatially limited. Recent advancements in remote sensing technologies now allow for rapid and large-scale estimation of flood-induced agricultural damage. This study assesses agricultural damage from two recent extreme flood events in Pakistan, integrating crop condition and flood intensity metrics. We present remote sensing-based case studies that employ an interdisciplinary approach, using Moderate Resolution Imaging Spectroradiometer (MODIS), Sentinel-1, and Sentinel-2 imagery along with crop data. Our results show that flood timing, crop stage, and inundation duration were the most influential factors in determining crop loss. We determined that Northern Sindh province and areas along the Indus River and its tributaries are highly vulnerable to flooding, resulting in extensive damage to infrastructure, crops, and loss of lives during flood events in 2010 and 2022, followed by Punjab, Balochistan, and Khyber Pakhtunkhwa. Remote sensing-derived damage estimates were closely aligned with post-event ground reports, validating the approach.

Keywords: flood; damage assessment; remote sensing; crop; loss assessment

check for updates

Academic Editors: Xinchun Cao, Guohua He, Qiong Yue and Mengyang Wu

Received: 14 September 2025
Revised: 19 October 2025
Accepted: 23 October 2025
Published: 25 October 2025

Citation: Nazir, A.; Ahmad, A.; Ramzan, M.; Gilani, H.; Mobeen, M.; Tarer, S.; Hanan, N.P. Flood-Induced Agricultural Damage Assessment: A Case Study of Pakistan. *Water* **2025**, *17*, 3060. https://doi.org/10.3390/w17213060

Copyright: © 2025 by the authors. Licensee MDPI, Basel, Switzerland. This article is an open access article distributed under the terms and conditions of the Creative Commons Attribution (CC BY) license (https://creativecommons.org/licenses/by/4.0/).

1. Introduction

Climate change directly impacts livelihood, food security, and agricultural yields [1], and the South Asian region is among the most severely affected regions, facing challenges like increasing annual average temperature as well as changes in rainfall patterns. Fatalities and food insecurity resulting from extreme weather like floods puts people in hazardous situations [2], with national governments and welfare organizations concerned about reducing casualties and other economic damage as flood disasters have become more frequent

and severe [3]. Flood frequency information on inundation and extent is required for assessing societal exposure, infrastructure destruction, economic losses, and crop damage [4]. Additionally, extreme flood events accelerate soil erosion, and siltation of rivers and dams, which have detrimental effects on soil fertility and agriculture.

Between 1998 and 2015, floods alone affected 2.3 billion people worldwide, with Asia accounting for the vast majority (95%) [5]. Globally, river flooding affects about 21 million people annually. However, numbers could rise to 54 million by 2030 due to climate change and socioeconomic growth [6]. Monsoon precipitation predominates in densely populated South Asia are spatially highly variable, contributing significantly to localized flooding [7–9] and significant crop losses, particularly in Pakistan and India [10,11]. Additionally, structural and economic losses occur due to recurrent floods in Bangladesh, northeastern India, and Nepal [12]. Previous work suggests that approximately 819 million people in India have experienced weather-related disasters between 1995 and 2015, followed by 127 million in Bangladesh [6], where 13 million people were affected by the 2007 floods, 36 million in 2004, 15 million in 1998, and 45 million people suffered from floods in 1988 [13]. Similarly, in Nepal in 2017, about 15,000 households were affected, with property losses estimated at 39 million dollars.

In Pakistan, according to recent estimates, the country suffered damages and economic losses of 30.2 billion US dollars from the floods of 2022, and another 16 billion US dollars will be required for rehabilitation [14]. The September 2020 flood in Karachi and across Sindh Province caused 34 casualties and affected 2 million people, including thousands of households [15]. The 2010 flood in Sindh, Punjab, and Khyber Pakhtunkhwa (KP) Provinces affected 21 million people, with almost 2000 casualties and an economic loss of $10 billion [16]. The agricultural sector in Pakistan is extremely vulnerable to climate change due to its geographical location and limited potential for adaptation [7,17], with Pakistan ranked globally as the 8th most adversely impacted country [18]. To provide food security for its rapidly expanding population, Pakistan is cultivating practically all its arable land [18] and in recent years, severe floods have resulted in significant agricultural losses [19], which destroyed 5.1 million acres of standing crops and seriously harmed more than 400,000 livestock [20], and highly destructive storms in 2018 and 2019 drastically reducing crop production in affected areas [21,22].

Remote sensing data offers potential for multi-resolution flood-inundation mapping and flood risk characterization [23], contributing to flood management preparation, prevention, and relief [24]. Compared to ground-based methods, space-based sensors provide near-real-time data for tracking the extent and severity of floods [25]. To monitor and evaluate the effects of floods across various river basins, several studies have used optical satellite data and related flood products [26,27]. However, several researchers underlined the value of Synthetic Aperture Radar (SAR) data in flood investigations, because SAR sensors can assess flood extent through clouds and heavy rain during flood and post-flood periods. SAR data are thus preferable in accurately distinguishing land and water in real-time flood damage assessment [28]. For example, studies of flood events in India and Bangladesh using Sentinel-1 have demonstrated the significant value of SAR data for flood extent mapping. However, the SAR sensor revisit interval (often 6–24 days) can limit its utility [29]. A combination of both optical and SAR data can enhance disaster monitoring ability.

The evaluation of post-disaster damages of floods is crucial given that catastrophic occurrences are becoming more frequent due to global warming. The evaluation of flood damages is also critical for post-disaster rehabilitation and recovery [30]. In the agricultural sector, flood damage assessments can support compensation procedures and aid in tracking and assessing the financial effects of disasters [31]. Remote sensing is an efficient technique

for analyzing loss and damage caused by natural catastrophes including floods, storms, and earthquakes. Synthetic Aperture Radar (SAR) satellite data can effectively map the extent of floods, especially in flood disasters [32] and optical satellites can be used to identify changes in vegetation cover before and after a flood in order to evaluate the damage caused by flooding [33]. Based on satellite imagery, researchers have created a variety of models and techniques to estimate floods and the losses that followed [34].

Flood and crop damage are commonly mapped using machine learning methods; however, this presents challenges because it requires a lot of processing power and training data. Conversely, NDWI is a straightforward method for removing surface water bodies; McFreeters [35] suggested a threshold value of zero, where all positive NDWI values are classified as water and negative values as non-water. Flood crop loss evaluation based on crop conditions primarily evaluated how the flood affected vegetation growth [36]. VIs served as the primary basis for these evaluations. Various methods were used, such as aggregating damaged areas based on remote sensing image bands, VIs thresholding, and comparing pre- and post-flood conditions [37]. Monitoring NDVI change in inundated cropland is a very straightforward method that makes the assumption that NDVI often decreases in crops damaged by flooding. To demonstrate the effect of the flood on crops, [38] compared NDVI time series with the historical median NDVI from 2000 to 2014. By contrasting the flooded year's spectral growth track with the typical crop growth track, flood damage was evaluated. The use of pricewise thresholding is necessary because crop responses vary depending on the crop-growing season, including vegetative, reproductive, mature, and ripening stages [36]. The threshold-based use of flood parameters is quite similar to the use of pricewise thresholding.

Proper identification of the flood and associated damages caused by recurring severe flooding events is critical to building resilience. Here, we explore the utility of both optical and SAR data for mapping flood extent and severity during two recent flood events in Pakistan, focusing on 2010 and 2022 floods [31]. This study's goals are to use SAR and optical data on the cloud platform Google Earth Engine (GEE) to explore (1) flood extent mapping and comparison between 2010 and 2022 at the district level, (2) crop damage assessment during the 2022 flood, and (3) pre- and post-flooding patterns of inundation during the 2010 and 2022 floods to assess the differential impact of these two major flood events on the agricultural sector of Pakistan. This study will help standardize reporting on losses connected to climate change, which will promote evidence-based policies for resilient reconstruction and food security for Pakistan.

2. Material and Methods

2.1. Study Area

Pakistan is the second largest South Asian country by area, the second most populous in South Asia, and fifth largest country by population in the world [39]. According to the Pakistan Bureau of Statistics, Pakistan was home to a population of 241.49 million people in 2017 [40], with 80% of the population dependent on agriculture for their livelihoods [21]. Among Pakistan's five main river systems (Jhelum, Sutlej, Ravi, Chenab, and Indus), the Indus River is the largest (Figure 1), providing irrigation water through a network of canals, distributaries, and watercourses [41]. Most of Pakistan's agricultural lands are in Punjab and Sindh Provinces, with agricultural systems producing crops such as wheat, cotton, rice, sugarcane, and maize, among other crops. The two main rainy seasons in Pakistan are defined as "Rabi", which spans October/November through April during cooler months and "Kharif" during the warm growing season months of May to September [41].

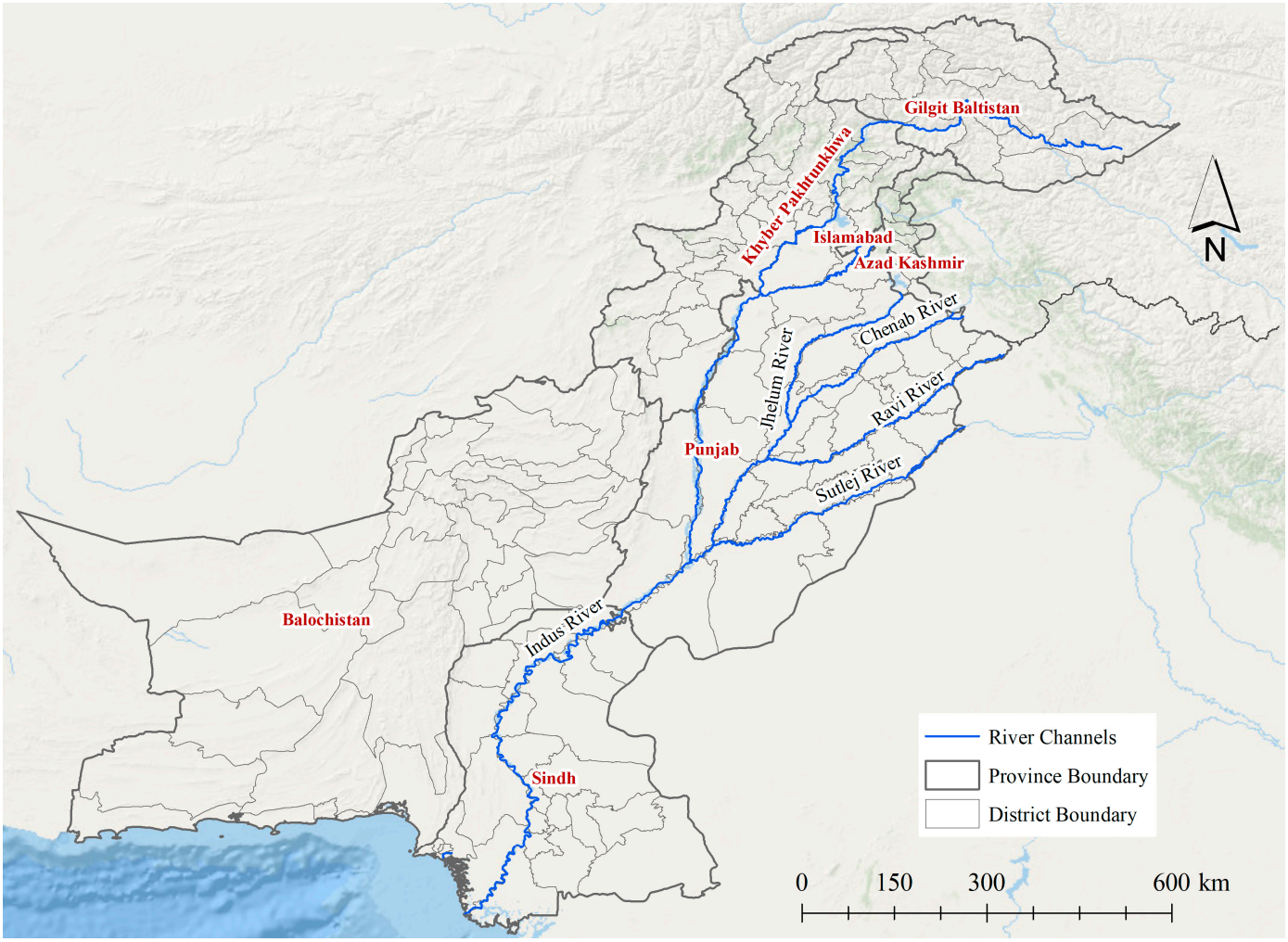

Figure 1. Study area map showing Pakistan's provinces and district boundaries and the primary river channels.

2.2. Satellite Data

2.2.1. Coarser Resolution Dataset

The MODIS terra surface reflectance product (MOD09A1.061) is utilized to map flood-affected areas during the 2010 and 2022 floods. The choice to include MODIS data in this analysis was based on several reasons. First, MODIS provides composite images with 8 days of interval including bands 1–7 at a resolution of 500 m and a swath size of about 2330 km compared to Landsat (revisit time of 16 days and a swath size of 185 km) [42,43]. This frequent revisit time is crucial for monitoring dynamic and rapidly changing flood events in near-real-time. Secondly, MODIS data is corrected for atmospheric conditions, including gases, aerosols, and Rayleigh scattering, making it easier to use with minimal preprocessing [44]. In addition to the seven reflectance bands, the product includes a quality layer and four observation bands. To determine the value for each pixel in 8, 15, and 30 days composite images, the algorithm selects the most suitable observation from all the acquisitions within the composite, considering factors such as high observation coverage, low view angle, absence of clouds or cloud shadows, and aerosol loading [44].

2.2.2. Medium Resolution Dataset

Sentinel-1 was used for 2022 flood inundation mapping. The Sentinel-1A and Sentinel-1B constellations are in a sun-synchronous, near-polar orbit. The flood-inundated area was located using data from the Sentinel-1 satellite's ground range detected (GRD) product,

which offered data in the C-band dual-polarization channels (VH and VV) with a 12-day temporal and 10 m spatial resolution. In August 2022, the Sentinel-1 images were processed in GEE to locate flooded pixels. Sentinel-2 (both A and B comprising a temporal resolution of 6 days) data is used for agriculture damage assessment during the post-flood period. Sentinel-2 is the best option for investigating plant phenology and tracking crop stress level, nutritional content, insect attack, and yield estimation due to the availability of numerous spectral bands in the red, near-infrared (NIR), and red edge regions of the electromagnetic (EM) spectrum with 10–20 m resolution [45]. Sentinel-2 compliments the MODIS data by providing a detailed analysis of post-flood damage to crop health and evaluation of vegetation stress.

2.3. Other Datasets

The European Space Agency's (ESA) land use land cover (LULC) dataset with 10 m resolution, produced for 2020 and 2021 (generated utilizing Sentinel-1 and Sentinel-2) and MODIS LULC for 2010 were used to extract the cropland and urban areas of Pakistan for flood damage assessment. The LULC product, developed as part of the ESA's 5th Earth Observation Envelope Program (EOEP-5) program, has 11 different land cover classifications [46]. JRC Global Surface Water Mapping Layers, v1.4 is utilized to map surface water's location and temporal distribution to exclude permanent water bodies when determining the extent of the flood [47]. Data related to affected population, fatalities, infrastructure, livestock, crops, and damage/loss to other sectors is acquired from the National Disaster Management Authority (NDMA) and Pakistan Bureau of Statistics (PBS) [48]. The NDMA in Pakistan was established in 2005 with the goal of enhancing the country's disaster management capacity. It is responsible for formulating policies, coordinating with provincial authorities, and improving resilience to disasters.

2.4. Methodology

The study is divided into two components: (1) flood inundation mapping, and (2) assessment of agricultural damage. (1) Flood inundation was assessed in four steps: (i) data collection, (ii) preprocessing data, which involves filtering clouds and noise, (iii) flood mapping using optical and SAR datasets, and (iv) flood masking, which includes post-processing to remove desert and hill shaded regions that were incorrectly mapped into the flood. Precipitation anomalies were calculated to indicate flood events. (2) The assessment of agricultural losses involves five steps: (i) data collection, (ii) preprocessing data, (iii) time series NDVI calculation, (iv) overlaying flood mask to quantify crop damage, and (v) validation. The flowchart (Figure 2) outlines the overall methodology employed in this analysis. The process is thoroughly explained in the sections that follow.

2.4.1. Flood Inundation Mapping 2010

Rainfall in Pakistan began episodically in July and persisted till August 2010, with large rainstorms coming in clusters on 19–21 July. The most intense rainfall occurred between 27 and 29 July, causing devastating floods at the start of August till late–mid-August. This was immediately followed by a period of moderate-to-heavy rain that persisted until mid-August. The MODIS product is employed in GEE for 2010 flood extent mapping. The surface reflectance bands 2 and 4 were utilized to compute the Normalized Difference Water Index (NDWI). The NDWI is a satellite imagery analysis technique that utilizes the near-infrared and visible green spectral bands to differentiate open water features [49]. The NDWI calculation is carried out using the following formula:

$$\mathrm{NDWI} = \frac{(\mathrm{Green} - \mathrm{NIR})}{(\mathrm{Green} + \mathrm{NIR})} \quad (1)$$

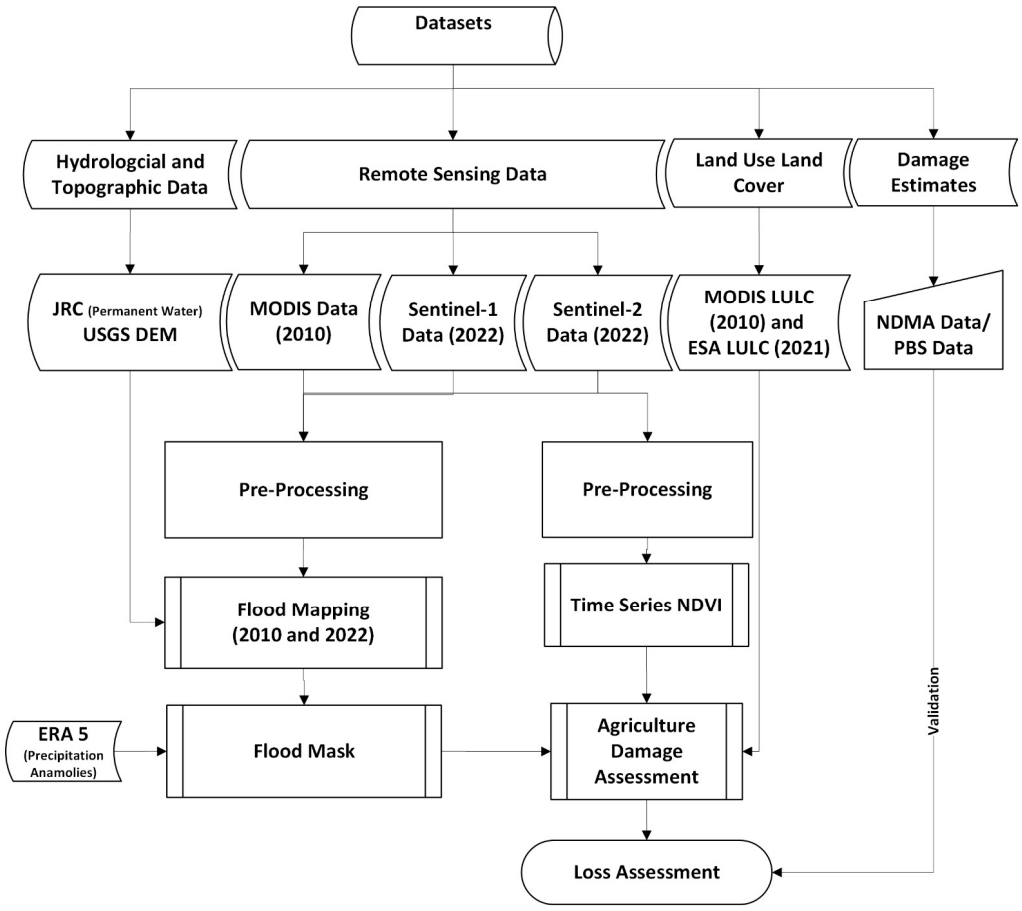

Figure 2. Flowchart illustrating the methodology employed in the analysis.

The NDWI ranges from −1 to 1, where 1 represents water bodies, while −1 represents dry areas or a lack of moisture [35]. Pre-flood NDWI in July and post-flood NDWI in September for both years, 2010 and 2022, were computed. The change detection technique is applied by subtracting the post-flood September NDWI image from the pre-flood image of July to acquire the areas affected by the floods.

2.4.2. Flood Inundation Mapping 2022

In July 2022, various locations in Pakistan experienced 15 days of rainfall, considered anomalous based on the climatological distribution. The floods intensified dramatically in late August (after 25 August) till mid-September, following a large rainfall storm from 17 to 25 August. Sentinel-1 imagery in the GEE data catalog is employed for 2022 flood mapping and is already pre-processed and analysis-ready. The usual pre-processing steps involve filtering images from Sentinel-1 data collection for the specified date that contains the study area and applying speckle filtering. The entire collection of Sentinel-1 images (from pre-flood to post-flood) was first filtered using standard approaches [50] including the pre- and post-flood date range from 15 August 2022, to 10 September 2022. We added a Lee speckle filter to reduce noise and a smoothing mean filter with a 50 m radius [51]. A thresholding technique is used to differentiate between flooded and non-flooded regions (threshold of −16 dB in VV polarization) [51].

The USGS provided the Digital Elevation Model (DEM) of 30 m resolution within the GEE data catalog for depth mapping and locating areas with a steep slope that had been mistakenly classified as flood water. The JRC, a global surface water layer, available on the GEE platform, was used to locate permanent and semi-permanent water bodies within the research region. The seasonality band with a spatial resolution of 30 m is utilized to map

and then exclude surface water bodies that are present for a maximum of 10 months in a year to accurately measure the flood extent of 2010 and 2022.

2.4.3. Crop and Infrastructure Damage Assessment

Sentinel-2 surface reflectance data is used to compute vegetation indices. Using GEE's "CLOUDY PIXEL PERCENTAGE" tool, we selected images from September to November of 2020 to 2022 with less than 10% cloud cover. The Sentinel-2 QA band was also employed to remove the clouds [52]. To isolate flood pixels, we utilized flood pixels computed from Sentinel-1 data. We extracted the cropland pixels that overlapped with the flood extent to determine the proportion of farmland area affected by flooding. Additionally, we employed the same procedure to extract the flooded built-up area. For the post-flood, vegetation health was calculated using Equation (2) and compared with crop health data from 2020 and 2021. Pixels falling within the healthy vegetation thresholds (NDVI > 0.5) were classified as non-flood damaged crops. Pixels lacking vegetation growth in the post-flood images but showing evidence of crop presence in pre-flood images were marked as damaged areas. Crop areas with low damage were identified based on crop regrowth during the post-flood period, although health remained lower than in previous years. The flood damage to crops is categorized into the following types: no damage (NDVI > 0.5), low damage (NDVI > 0.35 < 0.5), high damage (NDVI > 0.15 < 0.35), and complete damage (NDVI < 0.15), based on the extent of crop damage area (Figure S1). The category named "complete damage" represents areas that have been destroyed by floodwater. This process was repeated from September to November, and the common pixels were extracted for each class.

$$\mathrm{NDVI} = \frac{(\mathrm{NIR} - \mathrm{Red})}{(\mathrm{NIR} + \mathrm{Red})} \quad (2)$$

The NDVI ranges from -1 to 1, where 1 represents healthy vegetation, while -1 represents no vegetation.

Time series clustering was used to categorize different types of crops based on standard crop calendars (Table 1). Using 10 m spatial and 5-day temporal resolution Sentinel-2 satellite data, we assessed phenological development and related reflectance traits in multitemporal satellite data to identify crop types. The agricultural area is overlaid with the flood extent using AOI at the provincial and district levels, and crop type mask data at the district level to define the flood damage agricultural area and respective crop types. PBS's crop record is acquired for validating the crop areas for each district. The available LULC map is utilized to differentiate crop and non-crop areas. The GEE platform was utilized for data processing and analysis, R platform 4.5.0 for graphs and ArcGIS Pro 3.5.0 for post-processing and map making.

Table 1. Crop calendar of Pakistan major crops (Source: PMD).

Crop	Jan	Feb	Mar	Apr	May	June	July	Aug	Sep	Oct	Nov	Dec
Rice												
Sugarcane												
Cotton												
			Sowing				Growth				Harvesting	

3. Results

3.1. Precipitation Anomalies

Part of our analysis also focused on daily precipitation pattern monitoring to identify anomalies in rainfall patterns that may have contributed to floods in 2010 and 2022. We computed patterns during the monsoon months of July, August, and September for the years 2007, 2008, and 2009 and comparison with the corresponding months in 2010 (Figure 3).

Similarly, precipitation rates were computed in 2019, 2020, and 2021 and compared to 2022 (Figure 4). Visual inspection of the charts revealed several events of elevated precipitation in 2010, such as 12 mm on 21 July, the highest value of 26 mm on 28 July, 13 mm on 3 August, and 10 mm on 8 August. These persistent high values deviate from the established precipitation patterns of preceding years, although a notable peak of 15 mm was observed on 1 August 2008, as shown in Figure 3.

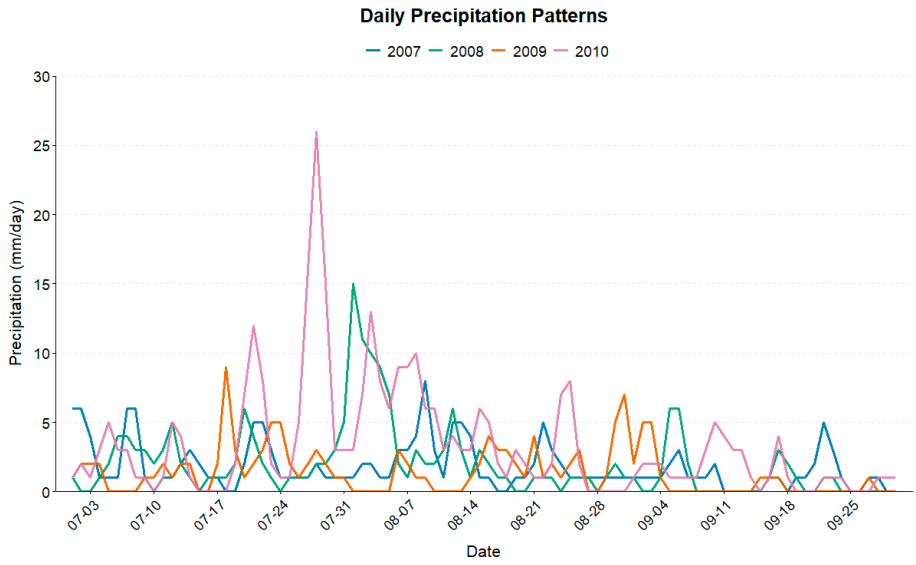

Figure 3. Precipitation anomalies during the flood 2010.

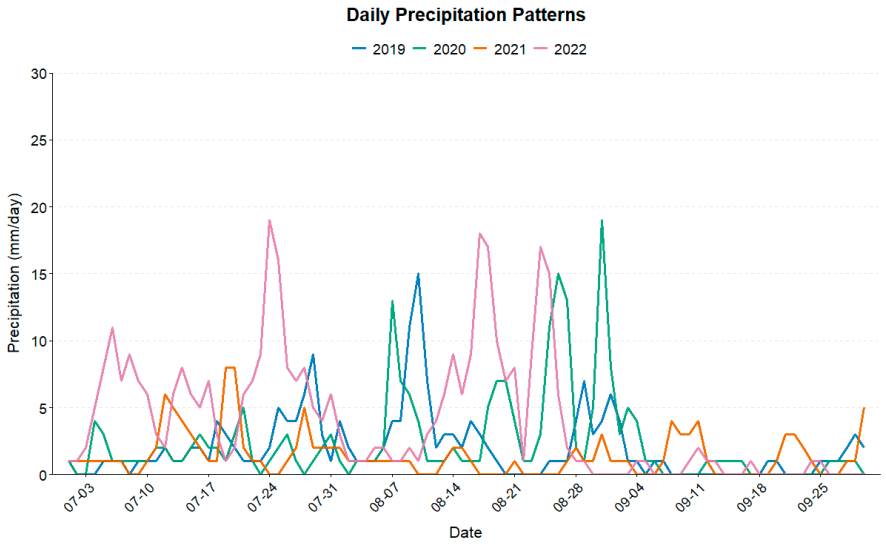

Figure 4. Precipitation anomalies during the flood 2022.

Analyzing the daily precipitation patterns of the previous three years from 2022, continuous elevated peaks were observed throughout July and the end of August in 2022. Noteworthy values include 11 mm on 6 July, 19 mm on 24 July, 18 mm on 17 August, 17 mm on 24 August, and 15 mm on 25 August (Figure 4). These high peaks differ significantly from the precipitation patterns of previous years. While higher precipitation levels were also recorded in 2020 and 2019, such as 19 mm on 31 August, followed by 15 mm on 26 August, and 13 mm on 7 August, the highest rainfall rate of 15 mm in 2019 occurred on 10 August (Figure 4). According to NDMA data, 249 casualties were reported in the September 2020 flood and 2 casualties in the September 2019 flood. The sustained high precipitation

rates from July to the end of August in 2022 likely contributed to the intense flooding in Pakistan.

3.2. Flood Inundation Mapping 2010 and 2022

We compared the 2010 and 2022 flood extent typically originated from the Indus River and its tributaries (Figure 5). We observed that the recent flood of 2022 was at a much larger scale when compared to the 2010 flood. In 2010, the flood primarily affected Sindh Province, with minor impacts observed in Punjab and Balochistan provinces. However, the 2022 flood significantly affected the Sindh and Punjab provinces, while minor impacts were observed in Balochistan and Khyber Pakhtunkhwa provinces (Figure 6).

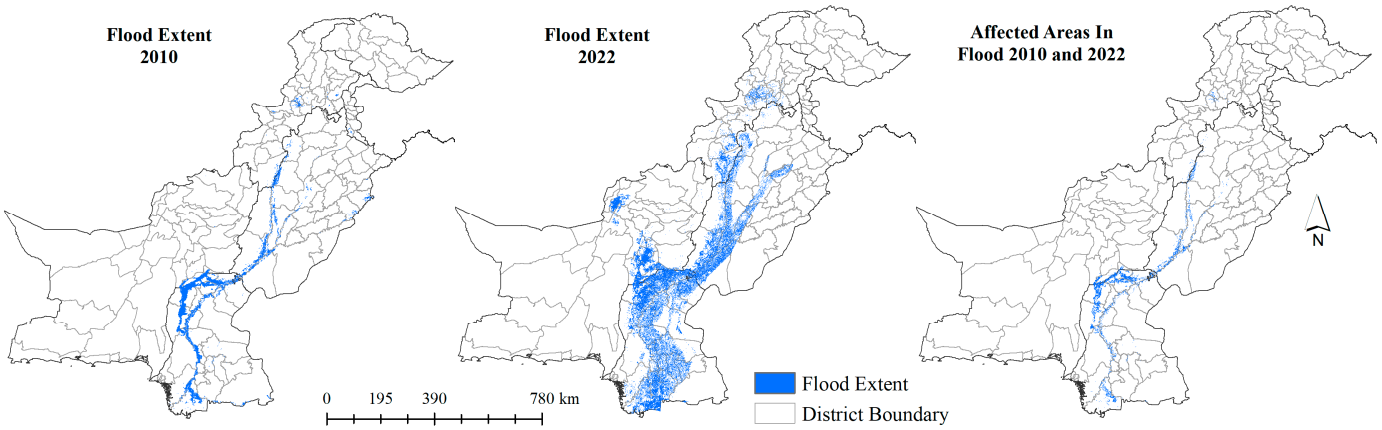

Figure 5. Flood extent assessment for 2010 and 2022 floods.

Flood extent areas for the years 2010 and 2022 were computed and compared across affected districts in the provinces of Balochistan, Khyber Pakhtunkhwa, Punjab, and Sindh. Notably, in Balochistan, the 2010 flood exhibited higher extents in Gwadar, Kech, and Awaran districts, covering areas of 3506 km^2, 2387 km^2, and 2063 km^2, respectively. In contrast, the 2022 flood showed reduced water extent, with maximum areas of 1407 km^2 and 1194 km^2 in Lehri and Nasirabad. In Khyber Pakhtunkhwa province, the 2010 flood displayed maximum extents in Dera Ismail Khan and Lakki Marwat, with areas of 697 km^2 and 417 km^2, respectively. In 2022, Dera Ismail Khan again experienced the highest flood extent, covering an area of 2100 km^2, followed by 520 km^2 in Lakki Marwat. In Punjab province, the 2010 flood recorded maximum extents in Rajanpur, Bhakkar, and Layyah, with affected areas of 1587 km^2, 1495 km^2, and 1242 km^2, respectively. In 2022, the maximum flood extents were observed in Rahim Yar Khan, Rajanpur, and Muzaffargarh, with areas of 3708 km^2, 3510 km^2, and 2704 km^2, respectively. Sindh experienced the 2010 flood with the maximum extent in Sujawal, covering 4039 km^2, followed by Jacobabad and Kambar Shadadkot with areas of 1597 km^2 and 1580 km^2, respectively. In 2022, Sujawal again witnessed the maximum flood extent, spanning 3758 km^2, followed by Kambar Shadadkot and Sanghar with areas of 2576 km^2 and 2492 km^2, respectively. Detailed statistics regarding flood extent areas for all affected districts within each province are given in Table 2.

Several districts of Sindh, Balochistan, Punjab, and Khyber Pakhtunkhwa districts were substantially affected by the flood inundation in August 2022 (Table 2). Punjab and Sindh's primary flood zones were the tributaries of the Indus, owing to breaching along the banks of the subsidiary rivers due to the heavy rainfall during the monsoon season. Khyber Pakhtunkhwa flood extent was primarily restricted to the vicinity regions of the Kabul River, and Balochistan flood extent was mainly restricted to the vicinity regions of

the Indus Tributary. Excessive flooding along the river Indus in Sindh is caused by the accumulated water flows from the Punjab and Khyber Pakhtunkhwa provinces. The Indus basin upstream portions had severe rainfall, leading to extreme flooding area (Figure 5). For instance, significant flood damage was caused in Sindh districts by flows from the Mari Bugti Hills, which were built in the plain region, creating a huge lake of flood inundation in the downslope lowlands immediately south of the plateau region. In all three regions (Punjab, Balochistan, and Khyber Pakhtunkhwa), the flood extent was at its maximum in August and at its lowest in October. In September and October, the area of the flood inundation decreased in Balochistan, Punjab, and Khyber Pakhtunkhwa. However, in Sindh, the flood water stands for a longer time.

Table 2. District-wise flood extent area (2010 and 2022).

Province	District	Flood 2010	Flood 2022	Province	District	Flood 2010	Flood 2022
Sindh	Badin	358	3343	Balochistan	Awaran	2063	-
	Dadu	1311	1619		Chagai	485	-
	Ghotki	279	2127		Dera Bugti	2	165
	Hyderabad	31	268		Gwadar	3506	-
	Jacobabad	1597	2092		Jaffarabad	780	887
	Jamshoro	674	643		Jhal Magsi	337	989
	Kambar Shahdadkot	1580	2576		Kachhi	11	467
	Kashmore	1049	1599		Kech	2387	-
	Khairpur	580	2343		Killa Abdullah	4	969
	Larkana	343	1116		Lasbela	582	3
	Matiari	264	629		Lehri	165	1407
	Mirpur Khas	-	1192		Mastung	-	200
	Naushahro Feroze	681	1399		Nasirabad	214	1194
	Sanghar	28	2492		Panjgur	410	-
	Shaheed Benazirabad	448	1618		Pishin	-	464
	Shikarpur	842	1502		Quetta	-	153
	Sujawal	4039	3758		Sibi	-	124
	Sukkur	639	1187		Sohbatpur	208	425
	Tando Allahyar	-	604		Washuk	854	-
	Tando Mohammad Khan	23	872	Punjab	Attock	34	216
	Tharparkar	427	91		Bahawalpur	20	507
	Thatta	950	457		Bhakkar	1495	943
	Umerkot	2	999		Chiniot	-	794
Khyber Pakhtunkhwa	Bannu	7	92		Dera Ghazi Khan	489	1329
	Buner	-	96		Hafizabad	-	80
	Charsadda	-	355		Jhang	936	912
	Dera Ismail Khan	697	2100		Jhelum	58	-
	Haripur	52	48		Khanewal	30	375
	Karak	41	85		Khushab	936	105
	Lakki Marwat	417	520		Layyah	1242	716
	Mardan	-	418		Mianwali	386	977
	Mirpur	70	-		Multan	139	1324
	Nowshera	15	134		Muzaffargarh	951	2704
	Peshawar	-	231		Rahim Yar Khan	668	3708
	Swabi	56	239		Rajanpur	1587	3510
	Tank	52	231		Sargodha	5	127

3.3. Crop and Infrastructure Damage Assessment

The analysis utilizing ESA Global Land Cover data revealed that the flood of 2022 had a detrimental effect on cropland and settlements (Table 3 and Figure S1). The province of Sindh experienced the highest level of impact affecting the cropland area of 20,914 km^2. In comparison, the damaged crop areas in Punjab, Balochistan, and Khyber Pakhtunkhwa were 5512, 5189, and 2761 km^2, respectively. Specifically, the flood of August 2022 caused damage to around 39.4% of agricultural areas in Sindh, 15.3% in Balochistan, and 14.9% in Khyber Pakhtunkhwa. However, Punjab has a lower percentage of affected cropland comparatively due to its higher altitude agricultural land area (Table 3).

For the assessment of crop impact in flood affected regions, major crops like sugarcane, rice, and cotton were taken into consideration, while minor crops such as maize and fodder were excluded. To estimate the extent of the flood from 1 August to 10 September 2022, Sentinel-1 data was utilized. Sentinel-2 data was used to generate rice, cotton, and sugarcane crop masks (an under-review study by Nazir et al., 2025) and determine their

affected areas. Additionally, PBS crop data was also utilized to assess crop's affected areas. The overall statistics at the provincial level can be found in Table 3. Among the provinces, Sindh has experienced the most significant impact on crops due to flood inundation, with 60% of the rice area in Sindh being damaged.

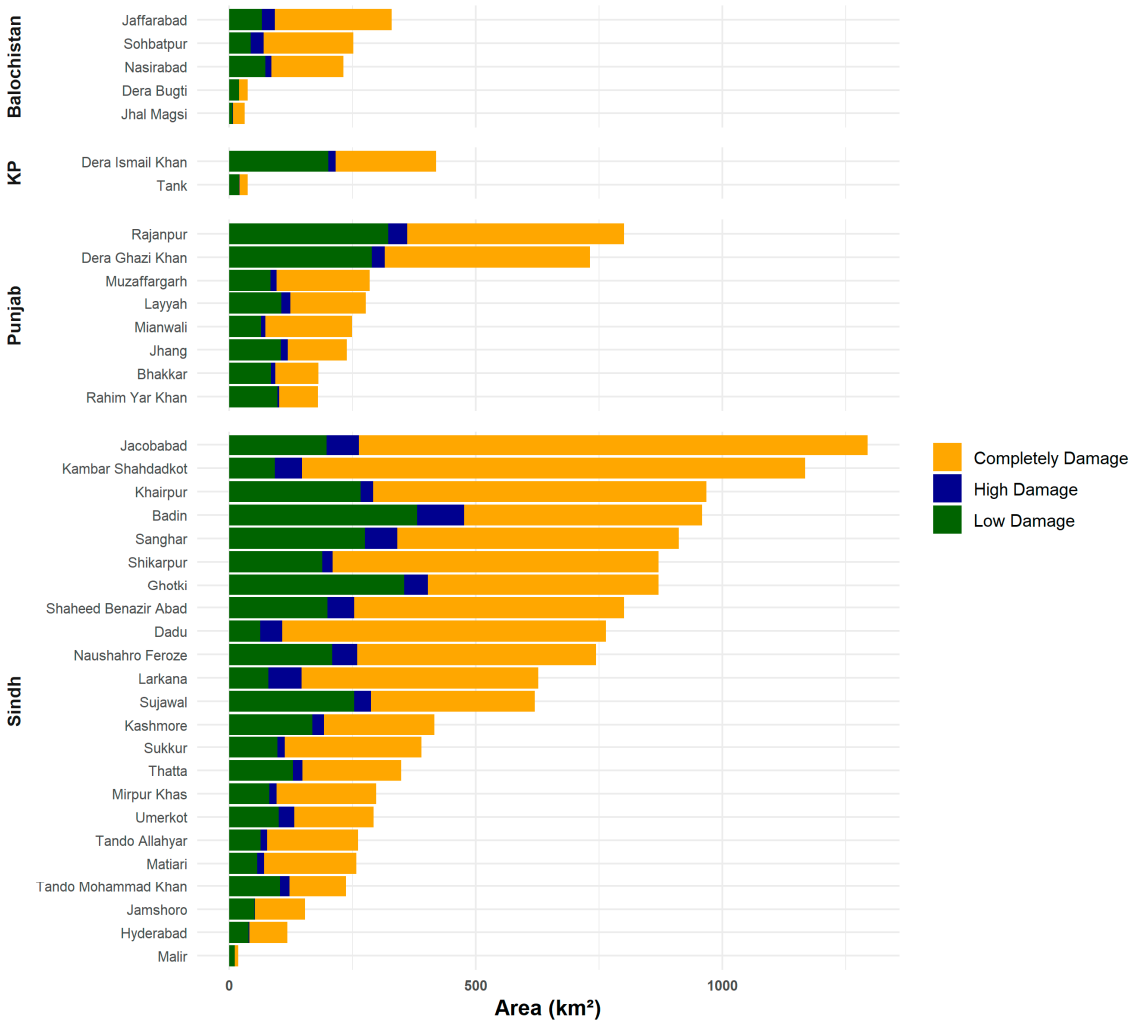

Figure 6. Crop damage area in various districts due to flood 2022.

Table 3. Damage to agricultural areas in various provinces of Pakistan during the 2022 flood.

Province/Region	Total Agriculture Area Utilizing ESA Land Cover 2021 (km^2)	Flood-Damaged Agriculture Area (km^2)	Flood-Damaged Agriculture Area Percentage (%)
Punjab	127,511	5512	4.3
Sindh	52,981	20,914	39.4
Khyber Pakhtunkhwa	18,481	2761	14.9
Balochistan	33,750	5189	15.3
Total	232,723	34,376	14.7

Sindh is the most highly affected province in terms of spatial extent and damage to crops among all the flood affected provinces of Pakistan. A total of 23 districts of Sindh were impacted by the flood. The highly affected districts were Jacobabad and Kambar Shahdadkot with 1032 and 1020 km^2 of crop damage area, respectively, followed by Khairpur with 676 km^2, Shikarpur with 661 km^2, Dadu with 656 km^2, Sanghar with 571 km^2, Shaheed Benazir Abad with 547 km^2, Naushahro Feroze with 484 km^2, Badin

with 482 km^2, Larkana with 480 km^2, Ghotki with 468 km^2, Sujawal with 332 km^2, Sukkur with 277 km^2, Kashmore with 223 km^2, Mirpur Khas with 202 km^2, Thatta with 200 km^2, Matiari with 187 km^2, Tando Allahyar with 185 km^2, Umerkot with 161 km^2, Jamshoro with 101 km^2, Hyderabad with 77 km^2, and Malir with 7 km^2. By combining all crop damage types, the highest flood-impacted districts of Sindh were Jocababad with a damaged crop area of 1295 km^2, followed by Kambar Shahdadkot with 1168 km^2, Khaipur with 968 km^2, Badin with 959 km^2, and Sanghar with 912 km^2. Various districts in Punjab have experienced crop damage due to flooding. The crops of Rajanpur identified as being completely damaged had an area of 440 km^2, followed by Dera Ghazi Khan with 416 km^2, Muzzafargarh with 189 km^2, Mianwali with 175 km^2, Layyah with 153 km^2, Jhang with 120 km^2, Bhakkar with 87 km^2, and Rahim Yar Khan with 78 km^2. Rajanpur and Dera Ghazi Khan are the highly affected districts of Punjab with 801 km^2 and 732 km^2 area when combining all levels of crop damage. Balochistan province was 3rd for damaged crop areas. Jaffarabad has been significantly affected, with a completely damaged crop area of 237 km^2, followed by Sohbatpur with 182 km^2, Nasirabad with 146 km^2, Jhal Magsi with 24 km^2, and Dera Bugti with 18 km^2. The most impacted districts of Balochistan were Jaffarabad, having a total crop damage area of 330 km^2, while the least damaged district was Dera Bugti with 38 km^2 of area. Khyber Pakhtunkhwa is ranked 4th, with Dera Ismail Khan and Tank being the most flood-impacted districts, with crop damage areas of 204 km^2 and 17 km^2, respectively.

4. Discussion

The Indus basin is extremely susceptible to flooding due to intense rainfall over shorter periods, resulting from climate change. Flood frequency and intensity have increased in recent decades among hydrometeorological risks due to climate change [7,51,53]. South Asia's mean annual temperature is rising [54], leading to changes in monsoon precipitation patterns, particularly in the Indus delta. Shared socio-economic pathway (SSP) simulations predict the higher risk of precipitation and extreme flooding during the monsoon season [55]. Satellite data may be extremely useful for impact assessment since it can be used to determine the primary extent of flooding and its effects on croplands and the urban population. In the current study, the flood extent assessment was carried out for the years 2010 and 2022 by identifying flood-inundated areas. The notable heavy precipitation during the monsoon months from July to September, particularly in 2010 and 2022, surpassed levels observed in preceding years. A comparative analysis revealed that the rates of precipitation during these two years exceeded those of the previous years (Figures 3 and 4). Consequently, it can be posited that the elevated precipitation witnessed in 2010 and 2022 played a pivotal role in causing the flooding events during these years. This underscores the correlation between intensified rainfall during the monsoon season and the occurrence of floods.

It is noteworthy to point out the significance of precise and high-resolution LULC information for flood inundation mapping and impact assessment. However, product-specific characteristics make LULC impact assessment challenging due to LULC variations across various products. For instance, the built-up class within MODIS-based LULC is underestimated, whereas ESRI's Sentinel-2 (10 m resolution)-based LULC shows an overestimation. In this scenario, we observe that the Copernicus LULC dataset from the ESA was useful for determining the damage to both the cropland and the build-up. Even though the ESRI LULC dataset is accessible at high resolution, the main drawback of this dataset over the Indus basin incorporates the riverbed region within the built-up class, which results in less precision in flood impact assessment. The disparity in the extent of impacted cropland observed in our study compared to other research [56] may

be attributed to the methodology employed. In the mentioned study, the assessment of cropland inundation relied solely on the global landcover product. However, in our evaluation, we adopted a more comprehensive approach by combining data from the global landcover product with the locally validated landcover dataset. This integration allowed us to achieve higher accuracy in our results, providing a more precise estimation of the actual cropland impacted by floods.

Significant variations in flood extent between the floods in Pakistan in 2010 and 2022, especially the change from northern to southern dominance, can be ascribed to a combination of environmental variables made worse by climate change, regional topography vulnerabilities, and unique meteorological drivers. A single upper-atmospheric storm that intensified monsoon rains over the steep Hindu Kush and Himalayas in 2010 caused riverine overflows along the Indus River and its tributaries. Province Sindh's land area was mainly submerged, following Punjab province due to the rapid runoff accelerated by the country's steep terrain. In contrast, the floods of 2022 flooded one-fifth of the country due to local rainfall and the Balochistan mountains' watersheds, causing significant inland flooding in northern Sindh, southern parts of Punjab, and eastern parts of Balochistan. These lowlands, which had poor drainage and heavy urban development on floodplains, stored water for prolonged periods of time, significantly increasing flood extent when compared to the fast-draining northern valleys in 2010. Crop damage increased with the length of the flood inundation in 2022. Additionally, rapid population growth and unchecked development in southern floodplains since 2010 are examples of anthropogenic factors that have increased vulnerability and contributed to the wider extent of inundation in 2022. In order to reduce future flood levels, these geographical differences highlight the necessity of specialized adaptation strategies, such as better drainage systems in southern plains and reforestation in northern catchments.

4.1. Flood 2010 Inundation Impact

The evaluation between the 2010 flood and the 2022 flood reveals significant differences in their impact on the affected population, fatalities, infrastructure, and economic losses (Tables S1–S3). In 2010, approximately 20 million people were affected, resulting in 1985 deaths, damage to 1.1 million houses, and the destruction of at least 436 healthcare facilities [57]. The impact of the floods on the rural economy was unprecedented, with significant damage to crops, livestock, animal sheds, personal seed stocks, fertilizers, agricultural machinery, fisheries, and forestry [58]. A highly affected sector was the agricultural sector, with 4.9 million acres of crops damaged and 1.2 million livestock lost, amounting to USD 10 billion in monetary damages [58]. Moreover, the floods led to an 80% loss of food reserves [59].

The United Nations Food and Agriculture Organization (FAO) reported that the 2010 floods impacted more than 180,000 km^2 of land, with over 16,000 km^2 of agricultural land affected. The FAO estimated that the floods destroyed or damaged around 16,000 km^2 of crops such as wheat, rice, maize, and sugarcane, leading to a loss of over 5 million tons of crops. Additionally, irrigation infrastructure, including canals and watercourses, was damaged, impacting crop cultivation and harvesting. The floods also had a detrimental impact on the livestock sector, with approximately 1.2 million animals lost, including cows, buffaloes, sheep, and goats, and animal shelters and feedstock damaged. The consequences of these losses were far-reaching, impacting the livelihoods of millions of rural farmers and communities [58]. The United Nations Development Program (UNDP) calculated the losses suffered by the agriculture sector at around USD 5.2 billion, including the cost of crop damage, loss of livestock, and damage to irrigation infrastructure and agricultural machinery. These figures indicate the severe consequences of the 2010 floods

on the agriculture sector in Pakistan, resulting in significant economic losses and negatively affecting the lives of millions of people.

4.2. Flood 2022 Inundation Impact

The Kabul Basin is a significant agricultural belt for the Balochistan province; the areas close to the river bodies are densely inhabited. In Balochistan, the population is more concentrated in the lower valley areas due to the reliance on river water. However, the population density in these areas remains relatively low compared to other regions within the study area. Sindh, on the other hand, has a significant population affected by flooding, primarily due to the presence of numerous tributary streams in densely populated areas. Sindh is greatly impacted by the numerous stream systems and the flow of river water from the Balochistan mountains, which causes chaos for the state throughout each monsoon season. Most of the flooded land was restricted to Sindh. Based on Sentinel-1 data, the calculated flood-inundated area during August 2022 was about 7450 km^2 (5.3%). The Indus basin was inundated by 19.48% (77,493.1 km^2) of the regions according to the composite flood maps during the 2022 flood event, with Sindh seeing the most inundation (5.3%), followed by Punjab (1.6%), Khyber Pakhtunkhwa (1.5%), and Balochistan (1.3%). The optical data (MODIS) obtained at the same time period as the SAR data, some of which are cloudy images, were used to compare the SAR-derived flood map to the false color composite (FCC) images. These findings demonstrate that the flood extent map corresponded to that seen in the optical FCC images and the gray-scale SAR data with accuracy. Moreover, these findings are in line with a recent report that found that the worst-affected districts in Sindh in 2022 were Jacobabad, Kambar Shahdadkot, Khairpur, Shikarpur, Dadu, Sanghar, and Nawabshah [60].

The physical impact of the floods in Pakistan was extensive, with a considerable percentage of households reporting damage to their homes. To accurately assess the severity of the flood hazard, it is necessary to consider the population estimate. According to [61], 54.8% of households suffered damage from floods, with more than half of them beyond repair. Furthermore, 28.8% of the households had significant but reparable damage, 10.9% experienced minor yet livable damage, and 5.6% had minimal damage. The floods also forced many households to leave, with 86.8% of households (76.9% urban vs. 88.3% rural) temporarily relocating for two weeks or more [61]. The economic consequences of the floods were also significant, adversely affecting the income of most households; ~88.0% of households (90.0% rural and 75.0% urban) experienced a decline in income. The average reported monthly income per household dropped significantly from less than 10,000 Rupees to less than 5000 Rupees [61]. Although fatalities and injuries directly linked to the floods were infrequent, the flood's aftermath had a significant impact on the health of those affected. Only a small percentage of households reported a flood-related injury (0.5%) or death (0.5%) [61]. During the six months following the flood, approximately 77.0% of households (71.1% urban vs. 76.5% rural) reported at least one member experiencing a health problem [61].

About 33 million people were impacted by the 2022 floods in Pakistan [48]. In total, 1739 casualties occurred, including 647 children, and 12,867 more were injured [48]. The number of houses lost or damaged increased to 1.7 million, indicating the severity of the flooding. The agricultural sector also experienced significant damage, with 8.3 million acres of crops affected and 1.1 million livestock lost. The economic losses amounted to USD 18 billion. This comparison underscores the increased scale and severity of the 2022 flood in terms of the affected population, fatalities, infrastructure damage, agricultural losses, and economic impact.

In terms of infrastructure and economy, around 897,014 homes were destroyed, while 1,391,467 were damaged [48]. Around 1,164,270 animals died, most of them in the province of Balochistan [48]. Access to the flood-affected areas has been hampered by damage to 439 bridges and 13,115 km (8149 miles) of roads [62]. More than 22,000 schools were destroyed or damaged [63]. Government authorities put the cost of economic damage and rehabilitation at least USD 30 billion, which is approximately 10% of Pakistan's GDP. Damages exceeded USD 14.9 billion, according to a needs assessment conducted by the Ministry of Planning, Development, and Special Initiatives in collaboration with the World Bank, the European Union (EU), the Asian Development Bank (ADB), and the United Nations agencies, with technical assistance from the United Nations Development Program (UNDP). Economic damage was estimated to be USD 15.2 billion, and it is predicted that at least USD 16.3 billion will be needed for rehabilitation and resilient building [64]. Resources are the main factor limiting the vulnerable groups' options for where to live in order to avoid dangerous locations [65]. Socially vulnerable populations may be more exposed to the effects of flood catastrophes because of their increased exposure [65].

5. Conclusions

This study demonstrates how cloud platforms such as Google Earth Engine (GEE) can facilitate large-scale inundation mapping across the Indus Basin using processed SAR and optical datasets. Such expansive flood mapping would not have been possible without the integration of remote sensing and cloud-based processing platforms. Our analysis show that flood events occur in August in Pakistan predominantly due to monsoon precipitation. Composite flood maps indicate that Sindh experienced the highest inundation (7500 km^2; 5.3% of its area), followed by Punjab (3300 km^2; 6.5%) due to their plain hierarchy of the terrain, Balochistan (4400 km^2; 1.26%), and Khyber Pakhtunkhwa (2100 km^2; 2.06%). These inundation events linked to intensifying climatic variability have significantly impacted agriculture (14.7% of farmland affected) and urban development (5.7–9.2% of built-up areas). As a direct consequence, millions of people were impacted by the floods, with Sindh suffering the most due to its residents' proximity to the river and lower valley. Northern Sindh province and areas along the Indus River and its tributaries are highly vulnerable to flooding, resulting in extensive damage to infrastructure, crops, and loss of lives during flood events in 2010 and 2022. Similarly, Punjab's high population and settlement density resulted in the highest impacts. Large-scale flood mapping was greatly aided by the SAR data, including crop damage assessment through Sentinel-2 data processing in the GEE platform and the resulting flood extent and crop damage maps. The findings support disaster managers and policymakers in developing targeted mitigation strategies and risk assessments by leveraging spatial data on affected croplands and population clusters. Future research should examine the institutional and socioeconomic obstacles to flood-resilient agriculture in southern Pakistan, assessing affordable approaches such as community-based early warning systems. For vulnerable agricultural systems, such studies can be included into national risk management frameworks to promote climate-adaptive policy with equitable recovery.

Supplementary Materials: The following supporting information can be downloaded at https://www.mdpi.com/article/10.3390/w17213060/s1, Table S1: Economic losses caused by flood 2022; Table S2: Damage and Loss to various sectors of Pakistan in 2022 flood; Table S3: Comparison of damages caused by 2010 and 2022 flood; Figure S1: Field validation of crops damaged by flooding. The recovered crop regions exhibited healthy vegetation, while the damaged crop regions showed no vegetation in Sentinel-2 imagery.

Author Contributions: Conceptualization, A.N., A.A., and M.R.; methodology, A.N., A.A., and H.G.; software, A.N.; validation, A.A., M.R., and H.G.; formal analysis, A.N.; investigation, A.N. and A.A.; resources, A.A. and M.R.; visualization, A.N., A.A. and M.M.; writing—original draft preparation, A.N.; writing—review and editing, A.N., H.G., S.T., M.M., M.R., and N.P.H.; supervision, H.G. and N.P.H. All authors have read and agreed to the published version of the manuscript.

Funding: This research received no external funding.

Data Availability Statement: The original contributions presented in this study are included in the article and Supplementary Materials. Raw data and further inquiries can be directed to the corresponding author.

Acknowledgments: We would like to express our thanks to the Savanna Lab and the management of the New Mexico State University (NMSU), NM, USA.

Conflicts of Interest: Authors Awais Ahmad and Shahid Tarer were employed by the company Kashtkaar, Pakistan. The remaining authors declare that the research was conducted in the absence of any commercial or financial relationships that could be construed as a potential conflict of interest.

References

1. Jiang, W.; Ji, X.; Li, Y.; Luo, X.; Yang, L.; Ming, W.; Liu, C.; Yan, S.; Yang, C.; Sun, C. Modified flood potential index (MFPI) for flood monitoring in terrestrial water storage depletion basin using GRACE estimates. *J. Hydrol.* **2023**, *616*, 128765. [CrossRef]
2. Harvey, C.A.; Saborio-Rodríguez, M.; Martinez-Rodríguez, M.R.; Viguera, B.; Chain-Guadarrama, A.; Vignola, R.; Alpizar, F. Climate change impacts and adaptation among smallholder farmers in Central America. *Agric. Food Secur.* **2018**, *7*, 57. [CrossRef]
3. Kuldeep; Garg, P.K.; Garg, R.D. Geospatial techniques for flood inundation mapping. In Proceedings of the 2016 IEEE International Geoscience and Remote Sensing Symposium (IGARSS), Beijing, China, 10–15 July 2016. [CrossRef]
4. Cohen, S.; Brakenridge, G.R.; Kettner, A.; Bates, B.; Nelson, J.; McDonald, R.; Huang, Y.F.; Munasinghe, D.; Zhang, J. Estimating Floodwater Depths from Flood Inundation Maps and Topography. *J. Am. Water Resour. Assoc.* **2018**, *54*, 847–858. [CrossRef]
5. The Human Cost of Weather-Related Disasters 1995–2015. Available online: https://www.undrr.org/publication/human-cost-weather-related-disasters-1995-2015 (accessed on 30 August 2025).
6. Centre for Research on the Epidemiology of Disasters (CRED). The Human Cost of Natural Disasters: A Global Perspective. 2015. Available online: https://www.preventionweb.net/publication/human-cost-natural-disasters-global-perspective (accessed on 14 June 2023).
7. Nazir, A.; Gilani, H.; Ramzan, M.; Hanan, N.P. Impacts of Extreme Floods on Agriculture in Pakistan. In Proceedings of the AGU Fall Meeting, Chicago, IL, USA, 12–16 December 2022; Available online: https://ui.adsabs.harvard.edu/abs/2022AGUFM.U25C2206N/abstract (accessed on 18 August 2025).
8. Kimuli, J.B.; Di, B.; Zhang, R.; Wu, S.; Li, J.; Yin, W. A multisource trend analysis of floods in Asia-Pacific 1990–2018: Implications for climate change in sustainable development goals. *Int. J. Disaster Risk Reduct.* **2021**, *59*, 102237. [CrossRef]
9. Trenberth, K.E.; Dai, A.; Rasmussen, R.M.; Parsons, D.B. The Changing Character of Precipitation. *Bull. Am. Meteorol. Soc.* **2003**, *84*, 1205–1218. [CrossRef]
10. Wang, J.; Li, K.; Hao, L.; Xu, C.; Liu, J.; Qu, Z.; Yan, X.; Sajjad, M.M.; Sun, Y. Disaster mapping and assessment of Pakistan's 2022 mega-flood based on multi-source data-driven approach. *Nat. Hazards* **2024**, *120*, 3447–3466. [CrossRef]
11. Ray, K.; Pandey, P.; Pandey, C.; Dimri, A.P.; Kishore, K. On the recent floods in India. *Indian Acad. Sci.* **2019**, *117*, 204–218. [CrossRef]
12. Dewan, T.H. Societal impacts and vulnerability to floods in Bangladesh and Nepal. *Weather Clim. Extrem.* **2015**, *7*, 36–42. [CrossRef]
13. Waghwala, R.K.; Agnihotri, P.G. Flood risk assessment and resilience strategies for flood risk management: A case study of Surat City. *Int. J. Disaster Risk Reduct.* **2019**, *40*, 101155. [CrossRef]
14. Baron, J.; Bend, M.; Roseo, E.; Farrakh, I. Floods in Pakistan. 2022. Available online: https://openknowledge.worldbank.org/entities/publication/c48738e5-715d-5566-8b98-25f16bb28cb3 (accessed on 14 June 2023).
15. Fihlani, P.; Mao, F. Pakistan floods: Monsoons bring misery to millions in Pakistan. *BBC News*, 26 August 2022. Available online: https://www.bbc.com/news/world-asia-62684037 (accessed on 30 August 2025).
16. NDMA Annual Report 2010. Available online: https://reliefweb.int/report/pakistan/ndma-annual-report-2010 (accessed on 17 June 2023).
17. Khan, S.; Sinha, R.; Whitehead, P.; Sarkar, S.; Jin, L.; Futter, M.N. Flows and sediment dynamics in the Ganga River under present and future climate scenarios. *Hydrol. Sci. J.* **2018**, *63*, 763–782. [CrossRef]

18. Syed, A.; Raza, T.; Bhatti, T.T.; Eash, N.S. Climate Impacts on the agricultural sector of Pakistan: Risks and solutions. *Environ. Chall.* **2022**, *6*, 100433. [CrossRef]
19. Fahad, S.; Wang, J. Farmers' risk perception, vulnerability, and adaptation to climate change in rural Pakistan. *Land Use Policy* **2018**, *79*, 301–309. [CrossRef]
20. Ministry of Water and Power, Government of Pakistan. Annual Flood Report 2012. Available online: https://ffc.gov.pk/wp-content/uploads/2020/06/Annual-Flood-Report-2012.pdf (accessed on 30 August 2025).
21. Elahi, E.; Khalid, Z.; Tauni, M.Z.; Zhang, H.; Lirong, X. Extreme weather events risk to crop-production and the adaptation of innovative management strategies to mitigate the risk: A retrospective survey of rural Punjab, Pakistan. *Technovation* **2022**, *117*, 102255. [CrossRef]
22. Khan, N.A.; Gao, Q.; Abid, M.; Shah, A.A. Mapping farmers' vulnerability to climate change and its induced hazards: Evidence from the rice-growing zones of Punjab, Pakistan. *Environ. Sci. Pollut. Res.* **2021**, *28*, 4229–4244. [CrossRef]
23. Sahoo, S.N.; Sreeja, P. Development of flood inundation maps and quantification of flood risk in an urban catchment of Brahmaputra River. *ASCE-ASME J. Risk Uncertain. Eng. Syst. Part A Civ. Eng.* **2015**, *3*, A4015001. [CrossRef]
24. Khan, S.I.; Hong, Y.; Wang, J.; Yilmaz, K.K.; Gourley, J.J.; Adler, R.F.; Brakenridge, G.R.; Policelli, F.; Habib, S.; Irwin, D. Satellite remote sensing and hydrologic modeling for flood inundation mapping in Lake Victoria basin: Implications for hydrologic prediction in ungauged basins. *IEEE Trans. Geosci. Remote Sens.* **2011**, *49*, 85–95. [CrossRef]
25. Cohen, S.; Raney, A.; Munasinghe, D.; Loftis, J.D.; Molthan, A.; Bell, J.; Rogers, L.; Galantowicz, J.; Brakenridge, R.; Kettner, A.J.; et al. The Floodwater Depth Estimation Tool (FwDET v2.0) for improved remote sensing analysis of coastal flooding. *Nat. Hazards Earth Syst. Sci.* **2019**, *19*, 2053–2065. [CrossRef]
26. Potcoava, M.C.; Stancalie, G.; Raducanu, D. The using of satellite image data from optic and microwaves data for development of a methodology for identification and extraction of flooded area. *Int. Arch. Photogramm. Remote Sens.* **2000**, *33*, 1185–1190.
27. Huang, M.; Jin, S. Rapid Flood Mapping and Evaluation with a Supervised Classifier and Change Detection in Shouguang Using Sentinel-1 SAR and Sentinel-2 Optical Data. *Remote Sens.* **2020**, *12*, 2073. [CrossRef]
28. Matgen, P.; Hostache, R.; Schumann, G.; Pfister, L.; Hoffmann, L.; Savenije, H.H.G. Towards an automated SAR-based flood monitoring system: Lessons learned from two case studies. *Phys. Chem. Earth Parts A/B/C* **2011**, *36*, 241–252. [CrossRef]
29. Das, P.; Chutiya, D.; Hazarika, N. Adjusting to Floods on the Brahmaputra Plains, Assam, India. 2009. Available online: https://lib.icimod.org/records/r39ae-wfp31 (accessed on 30 August 2025).
30. Schäfer, L.; Künzel, V. Steps Towards Closing the Loss & Damage Finance Gap Recommendations for COP25—First Version. Available online: https://www.germanwatch.org/sites/default/files/Policy%20Briefing_Steps%20towards%20closing%20the%20Loss%26Damage%20finance%20gap_0.pdf (accessed on 18 August 2025).
31. Qamer, F.M.; Abbas, S.; Ahmad, B.; Hussain, A.; Salman, A.; Muhammad, S.; Nawaz, M.; Shrestha, S.; Iqbal, B.; Thapa, S. A framework for multi-sensor satellite data to evaluate crop production losses: The case study of 2022 Pakistan floods. *Sci. Rep.* **2023**, *13*, 4240. [CrossRef] [PubMed]
32. Tay, C.W.J.; Yun, S.H.; Chin, S.T.; Bhardwaj, A.; Jung, J.; Hill, E.M. Rapid flood and damage mapping using synthetic aperture radar in response to Typhoon Hagibis, Japan. *Sci. Data* **2020**, *7*, 100. [CrossRef]
33. Tavus, B.; Kocaman, S.; Gokceoglu, C. Flood damage assessment with Sentinel-1 and Sentinel-2 data after Sardoba dam break with GLCM features and Random Forest method. *Sci. Total Environ.* **2022**, *816*, 151585. [CrossRef]
34. Dutta, D.; Herath, S.; Musiake, K. A mathematical model for flood loss estimation. *J. Hydrol.* **2003**, *277*, 24–49. [CrossRef]
35. McFeeters, S.K. The use of the Normalized Difference Water Index (NDWI) in the delineation of open water features. *Int. J. Remote Sens.* **1996**, *17*, 1425–1432. [CrossRef]
36. Rahman, M.S.; Di, L. A Systematic Review on Case Studies of Remote-Sensing-Based Flood Crop Loss Assessment. *Agriculture* **2020**, *10*, 131. [CrossRef]
37. Atefi, M.R.; Miura, H. Detection of Flash Flood Inundated Areas Using Relative Difference in NDVI from Sentinel-2 Images: A Case Study of the August 2020 Event in Charikar, Afghanistan. *Remote Sens.* **2022**, *14*, 3647. [CrossRef]
38. Shrestha, R.; Shao, Y.; Di, L.; Kang, L.; Yu, G.; Zhang, B. Detection of flood and its impact on crops using NDVI—Corn Case. In Proceedings of the 2013 2nd International Conference on Agro-Geoinformatics: Information for Sustainable Agriculture, Agro-Geoinformatics, Fairfax, VA, USA, 12–16 August 2013; pp. 200–204. [CrossRef]
39. Pakistan—The World Factbook. Available online: https://www.cia.gov/the-world-factbook/countries/pakistan/ (accessed on 12 September 2025).
40. MOIB. PBS Launches Results of 7th Population & Housing Census PAKISTAN. 18 July 2024. Available online: https://moib.gov.pk/News/62983 (accessed on 21 January 2025).
41. Nawaz, A.; Farooq, M.; Lal, R.; Rehman, A.; Hafeez-ur-Rehman. Comparison of conventional and conservation rice-wheat systems in Punjab, Pakistan. *Soil Tillage Res.* **2017**, *169*, 35–43. [CrossRef]
42. Landsat Science. Landsat 8. Available online: https://landsat.gsfc.nasa.gov/satellites/landsat-8/ (accessed on 12 September 2025).

43. MODIS Web. Available online: https://modis.gsfc.nasa.gov/ (accessed on 12 September 2025).
44. Erin, V. MODIS/Terra Surface Reflectance 8-Day L3 Global 500m SIN Grid V061 [Data Set]. NASA EOSDIS Land Processes DAAC. 2021. Available online: https://www.earthdata.nasa.gov/data/catalog/lpcloud-mod09a1-061 (accessed on 16 June 2023).
45. Narin, O.G.; Abdikan, S. Monitoring of phenological stage and yield estimation of sunflower plant using Sentinel-2 satellite images. *Geocarto Int.* **2022**, *37*, 1378–1392. [CrossRef]
46. Zanaga, D.; Van De Kerchove, R.; Daems, D. ESA WorldCover 10 m 2021 v200. 2022. Available online: https://zenodo.org/records/7254221 (accessed on 16 June 2023).
47. Pekel, J.F.; Cottam, A.; Gorelick, N.; Belward, A.S. High-resolution mapping of global surface water and its long-term changes. *Nature* **2016**, *540*, 7633. [CrossRef] [PubMed]
48. NDMA. NDMA Floods (2022): Sitrep Report No. 128. 19 October 2022. Available online: https://thedocs.worldbank.org/en/doc/4a0114eb7d1cecbbbf2f65c5ce0789db-0310012022/original/Pakistan-Floods-2022-PDNA-Main-Report.pdf (accessed on 30 August 2025).
49. Gao, B.C. NDWI—A normalized difference water index for remote sensing of vegetation liquid water from space. *Remote Sens. Environ.* **1996**, *58*, 257–266. [CrossRef]
50. Filipponi, F. Sentinel-1 GRD Preprocessing Workflow. *Proceedings* **2019**, *18*, 11. [CrossRef]
51. Loukas, A.; Garrote, L.; Vasiliades, L. Hydrological and Hydro-Meteorological Extremes and Related Risk and Uncertainty. *Water* **2021**, *13*, 377. [CrossRef]
52. Singha, M.; Dong, J.; Sarmah, S.; You, N.; Zhou, Y.; Zhang, G.; Doughty, R.; Xiao, X. Identifying floods and flood-affected paddy rice fields in Bangladesh based on Sentinel-1 imagery and Google Earth Engine. *ISPRS J. Photogramm. Remote Sens.* **2020**, *166*, 278–293. [CrossRef]
53. Fan, J.; Sun, W.; Zhao, Y.; Xue, B.; Zuo, D.; Xu, Z. Trend Analyses of Extreme Precipitation Events in the Yarlung Zangbo River Basin, China Using a High-Resolution Precipitation Product. *Sustainability* **2018**, *10*, 1396. [CrossRef]
54. Janes, T.; McGrath, F.; Macadam, I.; Jones, R. High-resolution climate projections for South Asia to inform climate impacts and adaptation studies in the Ganges-Brahmaputra-Meghna and Mahanadi deltas. *Sci. Total Environ.* **2019**, *650*, 1499–1520. [CrossRef] [PubMed]
55. Xiang, Y.; Wang, Y.; Chen, Y.; Zhang, Q. Impact of Climate Change on the Hydrological Regime of the Yarkant River Basin, China: An Assessment Using Three SSP Scenarios of CMIP6 GCMs. *Remote Sens.* **2022**, *14*, 115. [CrossRef]
56. Mushtaq, F.; Ali, M.; Ghosh, A.; Jalal, R.; Asghar, A.; Dadhich, G.; Chiozza, F.; Franceschini, G.; Muchoney, D.; Toirov, F.; et al. *A Rapid Geospatial Flood Impact Assessment in Pakistan 2022*; FAO: Rome, Italy, 2022.
57. WFP. Pakistan Flood Impact Assessment. September 2010. Available online: https://reliefweb.int/report/pakistan/pakistan-flood-impact-assessment-september-2010 (accessed on 17 June 2023).
58. FAO. Update on Agriculture—Pakistan Floods. 10 August 2010. Available online: https://www.fao.org/fileadmin/templates/tc/tce/pdf/Pakistan_Update_Agriculture_2.pdf (accessed on 17 June 2023).
59. Polastro, R.; Nagrah, A.; Steen, N.; Zafar, F. Inter-Agency Real Time Evaluation of the Humanitarian Response to Pakistan's 2010 Flood Crisis. 2011. Available online: https://daraint.org/wp-content/uploads/2011/03/Final-Report-RTE-Pakistan-2011.pdf (accessed on 16 June 2023).
60. Raza, S.I. Donors Pledge $500m for Flood Relief Efforts. 26 August 2022. Available online: https://www.dawn.com/news/1706855 (accessed on 14 June 2023).
61. Kirsch, T.D.; Wadhwani, C.; Sauer, L.; Doocy, S.; Catlett, C. Impact of the 2010 Pakistan Floods on Rural and Urban Populations at Six Months. *PLoS Curr.* **2012**, *4*, e4fdfb212d2432. [CrossRef] [PubMed]
62. Relief, I. Islamic Relief's Pakistan Floods Response 2022 (26 September, 2022). Available online: https://reliefweb.int/report/pakistan/islamic-reliefs-pakistan-floods-response-2022-26-september-2022 (accessed on 30 August 2025).
63. OCHA. PAKISTAN: 2022 Monsoon Floods. September 2022. Available online: https://reliefweb.int/report/pakistan/pakistan-2022-monsoon-floods-situation-report-no-5-9-september-2022 (accessed on 29 August 2025).
64. Altaf, M. Pakistan: Flood Damages and Economic Losses Over USD 30 billion and Reconstruction Needs Over USD 16 billion—New Assessment. *World Bank*, 28 October 2022. Available online: https://www.worldbank.org/en/news/press-release/2022/10/28/pakistan-flood-damages-and-economic-losses-over-usd-30-billion-and-reconstruction-needs-over-usd-16-billion-new-assessme (accessed on 17 June 2023).
65. Cutter, S.L.; Schumann, R.L., III; Emrich, C.T. Exposure, Social Vulnerability and Recovery Disparities in New Jersey after Hurricane Sandy. *J. Extrem. Events* **2014**, *1*, 1450002. [CrossRef]

Disclaimer/Publisher's Note: The statements, opinions and data contained in all publications are solely those of the individual author(s) and contributor(s) and not of MDPI and/or the editor(s). MDPI and/or the editor(s) disclaim responsibility for any injury to people or property resulting from any ideas, methods, instructions or products referred to in the content.